ISSN 1674-1056
http://cpb.iphy.ac.cn
http://iopscience.iop.org/cpb
中国物理 B
Chinese Physics
中国物理 Chinese Physics B

Lensless two-color ghost imaging from the perspective of coherent-mode representation

Bin Luo(罗斌), Guohua Wu(吴国华), Longfei Yin(尹龙飞)

Citation: Chin. Phys. B . 2018, 27(9): 094202. **doi:** 10.1088/1674-1056/27/9/094202

Journal homepage: http://cpb.iphy.ac.cn; http://iopscience.iop.org/cpb

What follows is a list of articles you may be interested in

Effect of atmospheric turbulence on entangled orbital angular momentum three-qubit state

Xiang Yan(闫香), Peng-Fei Zhang(张鹏飞), Jing-Hui Zhang(张京会), Xiao-Xing Feng(冯晓星), Chun-Hong Qiao(乔春红), Cheng-Yu Fan(范承玉)

Chin. Phys. B . 2017, 26(6): 064202. **doi:** 10.1088/1674-1056/26/6/064202

Noise analysis in ghost imaging from the perspective of coherent-mode representation

Bai Yan-Feng,Yang Wen-Xing,Yu Xiao-Qiang

Chin. Phys. B . 2012, 21(4): 044206. **doi:** 10.1088/1674-1056/21/4/044206

Second-order interference of two independent and tunable single-mode continuous-wave lasers

Jianbin Liu(刘建彬) Dong Wei(卫栋), Hui Chen(陈辉), Yu Zhou(周宇), Huaibin Zheng(郑淮斌), Hong Gao(高宏), Fu-Li Li(李福利), Zhuo Xu(徐卓)

Chin. Phys. B . 2016, 25(3): 034203. **doi:** 10.1088/1674-1056/25/3/034203

Photon counting statistics of V-type three-level systems: The effects of the field fluctuations

Peng Yong-Gang, Zheng Yu-Jun

Chin. Phys. B . 2015, 24(2): 024204. **doi:** 10.1088/1674-1056/24/2/024204

Correspondence normalized ghost imaging on compressive sensing

Zhao Sheng-Mei, Zhuang Peng

Chin. Phys. B . 2014, 23(5): 054203. **doi:** 10.1088/1674-1056/23/5/054203

Lensless two-color ghost imaging from the perspective of coherent-mode representation*

Bin Luo(罗斌)[1,†], Guohua Wu(吴国华)[2], and Longfei Yin(尹龙飞)[2]

[1] State Key Laboratory of Information Photonics and Optical Communications, Beijing University of Posts and Telecommunications, Beijing 100876, China
[2] School of Electronic Engineering, Beijing University of Posts and Telecommunications, Beijing 100876, China

(Received 9 March 2018; revised manuscript received 4 May 2018; published online 10 August 2018)

The coherent-mode representation theory is firstly used to analyze lensless two-color ghost imaging. A quite complicated expression about the point-spread function (PSF) needs to be given to analyze which wavelength has a stronger affect on imaging quality when the usual integral representation theory is used to ghost imaging. Unlike this theory, the coherent-mode representation theory shows that imaging quality depends crucially on the distribution of the decomposition coefficients of the object imaged in a two-color ghost imaging. The analytical expression of the decomposition coefficients of the object is unconcerned with the wavelength of the light used in the reference arm, but has relevance with the wavelength in the object arm. In other words, imaging quality of two-color ghost imaging depends primarily on the wavelength of the light illuminating the object. Our simulation results also demonstrate this conclusion.

Keywords: ghost two-color imaging, imaging quality, coherent-mode representation

PACS: 42.50.Ar, 42.25.Kb, 42.30.Va **DOI:** 10.1088/1674-1056/27/9/094202

1. Introduction

Ghost imaging is an indirect and nonlocal imaging method. The new imaging technique permits to image an object with single-pixel detector, which is realized by correlating the signals from two optical paths, the object arm and the reference arm. The object light which illuminates the object imaged is detected by a detector without any spatial resolution ability (a single-pixel detector or a bucket detector), and the reference light which does not usually interact with the object is detected by a spatial resolvable detector. The object information can be reconstructed by registering the intensity correlation as a function of the transverse position of the reference detector.

The realization of the imaging technique was attributed to quantum correlations associated with entangled photons generated by parametric down-conversion,[1–3] and the classically correlated light which is generated by illuminating a laser beam through a rotating ground class.[4–7] Recently, there have been many researches on new imaging schemes and methods. Ghost imaging technique combined with computer generated random patterns (computational ghost imaging),[8,9] sparsity constraints,[10,11] and compressive sensing[12,13] were investigated. Imaging through different circumstances, including turbulent atmosphere,[14–16] scattering media,[17–19] turbid media,[20] and refractive media,[21] were studied. Ghost imaging with the reflective targets were analyzed theoretically and experimentally.[22–24] The scheme of ghost imaging lidar which can be used in the field of remote sensing was also proposed.[10,25–28]

Note that the most work focused on ghost imaging with monochromatic thermal light. Recently, some works have discussed two-color, even multi-wavelength ghost imaging.[29–32] Chan *et al.* firstly studied two-color ghost imaging using either thermal or quantum light sources. Their results showed that the resolution of two-color thermal ghost imaging can be higher than its quantum counterpart. By a very complicated point-spread function (PSF), they also showed that the spatial resolution of ghost-image depends primarily on the wavelength used to illuminate the object.[29] A new coherent-mode representation theory was reported to analyze ghost imaging with classical light source, and the results showed that this theory is suitable for evaluating imaging quality in $2f$, f–$2f$, and lensless Fourier-transform ghost imaging systems.[33] We discussed the possibility that the theory is used in a ghost microscope imaging system.[34] However, whether the coherent-mode representation can be used to analyze lensless two-color ghost imaging is not mentioned in these works.

In this paper, we investigate lensless two-color ghost imaging by using the coherent-mode representation theory. It is shown that the intensity fluctuation correlation function in a lensless two-color ghost imaging system can be changed from the usual two-dimensional integral representation to a new one-dimensional summation representation, based on which imaging quality can be analyzed by the distribution variety of the decomposition coefficients of the object imaged. By the analytical and numerical results, we show that the decomposi-

*Project supported by the National Natural Science Foundation of China (Grant Nos. 61771067, 61631014, 61471051, and 61401036) and the Youth Research and Innovation Program of Beijing University of Posts and Telecommunications, China (Grant Nos. 2015RC12 and 2017RC10).

†Corresponding author. E-mail: luobin@bupt.edu.cn

© 2018 Chinese Physical Society and IOP Publishing Ltd

tion coefficients are only related to the wavelength used in the object arm. The theory is quite suitable for evaluating which wavelength has a stronger effect on imaging quality in two-color ghost imaging.

2. Model and analytical results

To demonstrate two-color ghost imaging, a conventional lensless ghost imaging system with pseudothermal light needs minor modification, as shown in Fig. 1. A laser beam composed of two different wavelengths λ_1 and λ_2 passes through a spatial light modulating system (SLMS). The system can impress identical random intensity patterns onto the two-color light to produce the pseudothermal source, and then the modulated light is divided by a dichroic mirror (DM) as two beams. In the object arm (λ_1), an object (with the transmission function $t(x')$) is placed at a distance z_1 from the source and a CCD camera 1 is placed at a distance z_2 from the object. In the reference arm (λ_2), only a CCD camera 2 is placed at a distance z from the source. The impulse response functions for the two arms can be expressed as

$$h_1(x_1,u_1) = \int \frac{\mathrm{e}^{-\mathrm{i}k_1 z_1}}{\mathrm{i}\lambda_1 z_1}\exp\left[\frac{-\mathrm{i}\pi}{\lambda_1 z_1}(x'-x_1)^2\right]t(x') \times \frac{\mathrm{e}^{-\mathrm{i}k_1 z_2}}{\mathrm{i}\lambda_1 z_2}\exp\left[\frac{-\mathrm{i}\pi}{\lambda_1 z_2}(u_1-x')^2\right]\mathrm{d}x', \quad (1)$$

$$h_2(x_2,u_2) = \frac{\mathrm{e}^{-\mathrm{i}k_2 z}}{\mathrm{i}\lambda_2 z}\exp\left[\frac{-\mathrm{i}\pi}{\lambda_2 z}(u_2-x_2)^2\right]. \quad (2)$$

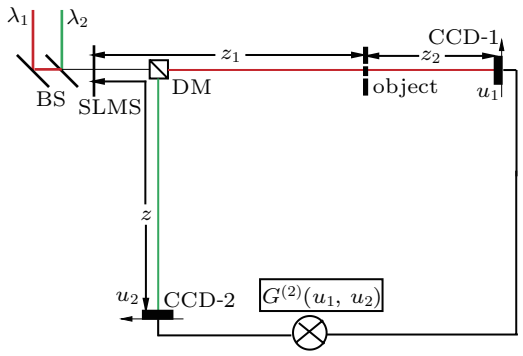


Fig. 1. (color online) A simplified scheme for lensless two-color ghost imaging.

The information of the object can be retrieved by measuring intensity fluctuation correlation function[6]

$$G(u_1,u_2) = \langle \Delta I_1(u_1)\Delta I_2(u_2)\rangle = \left|\int \Gamma(x_1,x_2)h_1^*(x_1,u_1)h_2(x_2,u_2)\mathrm{d}x_1\mathrm{d}x_2\right|^2, \quad (3)$$

where $\Delta I_i(u_i) = I_i(u_i) - \langle I_i(u_i)\rangle$ $(i=1,2)$ and $\Gamma(x_1,x_2)$ is the second-order correlation function of the source.

Based on the second-order coherence theory of optical fields, $\Gamma(x_1,x_2)$ can be expressed in the coherent-mode representation[35] as

$$\Gamma(x_1,x_2) = \sum_n \beta_n \phi_n^*(x_1)\phi_n(x_2), \quad (4)$$

where β_n and ϕ_n are the corresponding eigenvalues and eigenfunctions of the homogeneous Fredholm integral equation, and

$$\int \Gamma(x_1,x_2)\phi_n(x_1)\mathrm{d}x_1 = \beta_n\phi_n(x_2). \quad (5)$$

Substituting Eq. (4) into Eq. (3) and using Eq. (5), $G(u_1,u_2)$ can be rewritten as

$$G^{(2)}(u_1,u_2) = \left|\sum_n \beta_n f_n^*(u_1)g_n(u_2)\right|^2, \quad (6)$$

with

$$\begin{cases} f_n(u_1) = \int h_1(x_1,u_1)\phi_n(x_1)\mathrm{d}x_1, \\ g_n(u_2) = \int h_2(x_2,u_2)\phi_n(x_2)\mathrm{d}x_2, \end{cases} \quad (7)$$

and

$$\begin{cases} h_1(x_1,u_1) = \sum_n f_n(u_1)\phi_n^*(x_1), \\ h_2(x_2,u_2) = \sum_n g_n(u_2)\phi_n^*(x_2). \end{cases} \quad (8)$$

By using Eq. (6), Cheng and Han discussed the possibility that the coherent-mode representation theory is used to analyze ghost-image in three ghost imaging schemes ($2f$, f–$2f$, and lensless Fourier-transform ghost imaging systems), and their results showed that the theory is very suitable for evaluating imaging quality.[33] Note that their discussion did not include lensless ghost imaging, and the light source used in their work is monochromatic. In the following, we focus on the possibility that lensless two-color ghost imaging is studied by the coherent-mode representation theory.

First, substituting Eq. (1) into Eq. (8) and considering $z_1 = z$, we can obtain

$$t^*(u_1) = \sum_n f_n^*(u_1)\int \phi_n(x_1)\exp\left[\frac{-\mathrm{i}\pi}{\lambda_1 z}(u_1-x_1)^2\right]\mathrm{d}x_1, \quad (9)$$

where z_2 in Eq. (1) is ignored. f_n^* can be looked upon as the decomposition coefficients of the object imaged.

Then, substituting Eq. (1) into Eq. (7), we have

$$g_n(u_2) = \int \phi_n(x_2)\exp[-\mathrm{i}\pi(u_2-x_2)^2/(\lambda_2 z)]\mathrm{d}x_2.$$

After considering the above equation, equation (6) can be rewritten as

$$G(u_1,u_2) = \left|\sum_n \beta_n f_n^*(u_1)\int \phi_n(x_2) \times \exp\left[\frac{-\mathrm{i}\pi}{\lambda_2 z}(u_2-x_2)^2\right]\mathrm{d}x_2\right|^2. \quad (10)$$

If we choose a Gaussian Schell-model source, β_n and ϕ_n are the corresponding eigenvalue and eigenfunction of the coherent-mode representation of the light source,[35] and

$$\beta_n = \left(\frac{\pi}{a+b+c}\right)^{1/2}\left(\frac{b}{a+b+c}\right)^n,$$

$$\phi_n(x) = \left(\frac{2c}{\pi}\right)^{1/4} \frac{1}{\sqrt{2^n n!}} \mathrm{H}_n(x\sqrt{2c}) \mathrm{e}^{-cx^2}, \qquad (11)$$

where $a = 1/4\sigma_1^2$, $b = 1/2\sigma_g^2$, and $c = \sqrt{a^2 + 2ab}$. σ_1 is the diameter of the laser beams illuminating the SLMS, σ_g represents the size of the spatial correlations of the two beams at the out plane of the SLMS, and $\mathrm{H}_n(x)$ are the Hermite polynomials. Here, we consider the situation of $\lambda_i < \sigma_g \ll \sigma_1$.[29]

By comparing Eq. (10) with Eq. (9), the object's transmission function can be perfectly imaged under the condition of $\beta_n = \beta_0$ and $\lambda_1 = \lambda_2$. From Ref. [33], imaging quality depends crucially on the distribution of β_n and f_n. It is shown that from Eq. (11) β_n is only related with the properties of the source (the transverse size and the transverse coherence width). We will keep the two parameters unchanged in the following discussion, so the effect of β_n on imaging quality can be ignored. In other words, the change of imaging quality is primarily due to the wavelength difference $\lambda_1 \neq \lambda_2$. From Eqs. (1) and (7), the variety of the wavelength can influence the distribution of f_n, and thus affect imaging quality. It is also noted that f_n only concerns the wavelength used in the object arm, and has no relation with the one in the reference arm, so imaging quality of two-color ghost imaging depends primarily on the wavelength of the light illuminating the object.

3. Simulation results

In this section, we give the numerical simulations to demonstrate the above analytical results. During the process, a double-slit with the slit width 0.08 mm and the distance between two slits 0.16 mm is chosen as the object imaged, and the parameters of light source are fixed as $\sigma_1 = \sqrt{1/4a} = 4.0$ mm and $\sigma_g = \sqrt{1/2b} = 0.06$ mm. A further point that should be noted is that an imaging detector instead of a point-like detector is used in the test arm, so the ghost-image should be defined as $G^{(2)}(u_2) = \int G^{(2)}(u_1, u_2)\mathrm{d}u_1$.

We firstly consider the case of the monochromatic light source $\lambda_1 = \lambda_2 = 532$ nm. Figures 2(a) and 2(b) show the distribution of the eigenvalues β_n of the coherent-mode representation of the source and the decomposition coefficients f_n of the object, respectively. The reconstructed image (the upper) over 10000 CCD frames and its cross-section curve (the bottom) are presented in Fig. 2(c). According to the conclusion in Ref. [33], high quality ghost images can be obtained when the distribution of β_n is wider than the distribution of f_n, i.e., increasing the distribution of β_n or decreasing the distribution of f_n can result in the improvement of imaging quality. From Figs. 2(a) and 2(b), f_n has a relative narrow distribution when compared with the distribution of β_n, which will result in good imaging quality, as shown in Fig. 2(c).

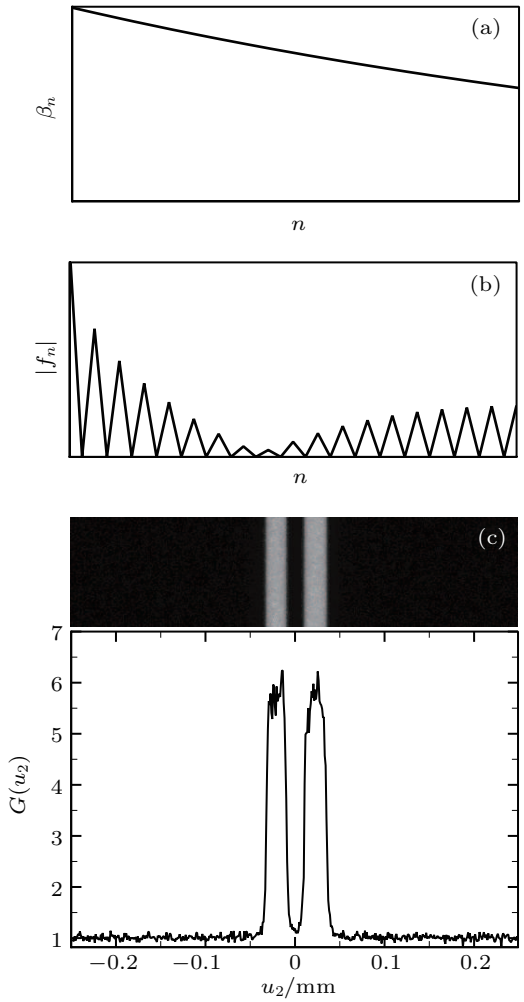


Fig. 2. (a) The first 50 eigenvalues of the coherent-mode representation of the source. (b) The first 50 decomposition coefficients of the object. (c) The reconstructed image of the double-slit (statistics over 10000 CCD frames) (the upper) and its cross-section curve (the bottom). The parameters are chosen as $\sigma_1 = \sqrt{1/4a} = 4.0$ mm, $\sigma_g = \sqrt{1/2b} = 0.06$ mm, $n = 50$, $z_1 = z = 175$ mm, and $\lambda_1 = \lambda_2 = 532$ nm.

To show how two-color light source affects imaging quality when compared with the monochromatic light, we first change the wavelength in the object arm but keep the wavelength in the reference arm unchanged. Here we choose two different λ_1 values 546 nm and 560 nm, and the corresponding results are shown in Figs. 3(a) and 3(b), respectively. The distribution of the eigenvalues β_n of the coherent-mode representation of the source does not be shown because it is only related with a (σ_1) and b (σ_g), and its distribution has no changes in the following discussion when the parameters of the source keep unchanged. The distribution changes of the decomposition coefficients of the object are not obvious when the wavelength λ_1 is increased slightly. To show clearly this variety, we give the difference between f_n when the two-color light source is used and that with the monochromatic light, and magnify the difference ten times. Clearly, the distribution of f_n increases with an increase of λ_1, which will lead to the decline of imaging quality. From Figs. 3(a2) and 3(b2), the imaging quality gradually gets worse with the increase of λ_1 when compared with the

case with the monochromatic light source in Fig. 2(c), which is consistent with our prediction according to the distribution change of f_n.

To get a deeper insight into the effect from the wavelength change in the object arm on the imaging quality, we depict the dependence of the fidelity on the wavelength difference λ_1–λ_2 in Fig. 3(c). Here the fidelity is defined as $R = \int U(x)U_C(x)\mathrm{d}x/\sqrt{(\int U(x)\mathrm{d}x)^2(\int U_C(x)\mathrm{d}x)^2}$,[36] where $U(x)$ denotes the image from two-color ghost imaging and $U_C(x)$ presents the image obtained from ghost imaging with the monochromatic light. The value of R can range from 0 to 1, and the bigger the R value is, the higher the similarity degree between the two images is. From Fig. 3(c), the fidelity declines when the wavelength in the object arm increases, and the change is more and more obvious with an increase of the wavelength difference.

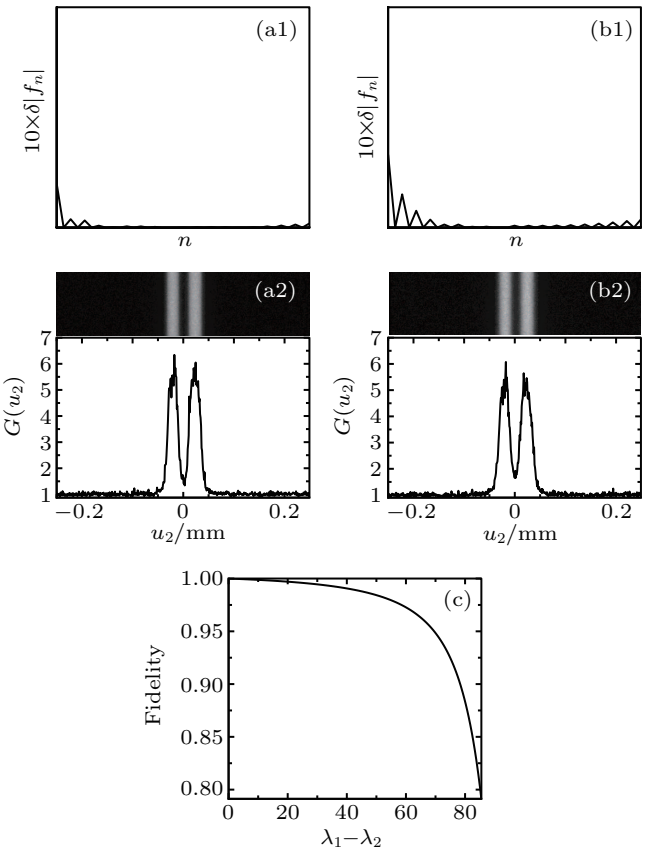


Fig. 3. (a) The distribution difference of f_n which is magnified ten times when λ_1 is increased from 532 nm to 546 nm (upper left) and the reconstructed image (bottom left). (b) The case for $\lambda_1 = 560$ nm. Other parameters are the same as those in Fig. 2. (c) The fidelity versus the wavelength difference.

Then we analyze the effect from the wavelength of the light used in the reference arm, and the results are plotted in Fig. 4. During this process, the wavelength in the object arm keeps unchanged. The distribution variety of the decomposition coefficients of the object do not be shown because f_n is not related with λ_2, as shown in Eqs. (1) and (7). In other words, the change of λ_2 does not influence the distribution variety of f_n. So imaging quality almost has no changes, as shown in Fig. 4. The relationship between the fidelity and the wavelength difference by increasing the wavelength in the reference arm is plotted in Fig. 4(c). The result is quite different from that in Fig. 3(c). The value of the fidelity keeps unchanged for a small change of the wavelength in the reference arm, which agrees with the results shown in Figs. 4(a) and 4(b). However, the fidelity decreases for a large $\lambda_1 - \lambda_2$ value, and it is shown that the fidelity by changing λ_2 is always smaller than that by increasing λ_1.

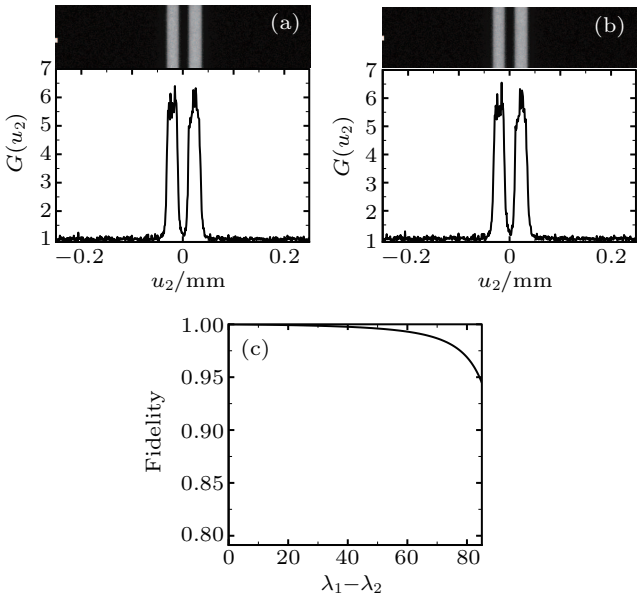


Fig. 4. The reconstructed double-slit for (a) $\lambda_2 = 546$ nm and (b) $\lambda_2 = 560$ nm. Other parameters are the same as those in Fig. 2. (c) The fidelity versus the wavelength difference.

By comparing Figs. 3 and 4, imaging quality in a lensless two-color ghost imaging system depends primarily on the wavelength used in the object arm. One has to give a quite complicated expression about PSF to explain this phenomenon when the usual integral representation theory is used.[29] Here it is shown that the change of wavelength in the object arm λ_1 results in the distribution variety of the decomposition coefficients of the object f_n, which finally leads to the change of imaging quality. While the wavelength in the reference arm λ_2 does not have a similar impact because f_n is not related with λ_2. In other words, the coherent-mode representation theory is quite suitable for analyzing which wavelength has a stronger impact on imaging quality in two-color ghost imaging. It is also noted that imaging quality will have some changes when the wavelength change in the reference arm is quite big.[31] So the theory is only suitable for the case with small variety of light wavelength in the reference arm. How to improve the theory under the big wavelength change will be discussed in our future work.

4. Conclusion

We have investigated the possibility of analyzing imaging quality in a lensless two-color ghost imaging system by the coherent-mode representation theory. Unlike the integral representation theory under which one has to give a complicated expression of PSF to study which wavelengths has a bigger influence on imaging quality in a two-color ghost imaging, from the coherent-mode representation, one can investigate imaging quality of two-color ghost imaging by the distribution variety of the decomposition coefficients of the object which is caused by the wavelength changes. The analytical and numerical results show that the distribution variety of f_n is only related to the wavelength in the object arm. In other words, imaging resolution depends primarily on the wavelength of the light illuminating the object. We also analyze the applicable condition of the coherent-mode representation theory. It should be emphasized that the two-color light source used in this paper is produced by using SLMS, and it is an artificial and controllable source. In other words, our results are not suitable for the true thermal light source.

References

[1] Strekalov D V, Sergienko A V, Klyshko D N and Shih Y H 1995 *Phys. Rev. Lett.* **74** 3600
[2] Pittman T B, Shih Y H, Strekalov D V and Sergienko A V 1995 *Phys. Rev. A* **52** R3429
[3] Barbosa G A 1996 *Phys. Rev. A* **54** 4473
[4] Bennink R S, Bentley S J and Boyd R W 2002 *Phys. Rev. Lett.* **89** 113601
[5] Gatti A, Brambilla E, Bache M and Lugiato L A 2004 *Phys. Rev. A* **70** 013802
[6] Cheng J and Han S 2004 *Phys. Rev. Lett.* **92** 093903
[7] Cao D Z, Xu B L, Zhang S H and Wang K G 2015 *Chin. Phys. Lett.* **32** 114208
[8] Shapiro J H 2008 *Phys. Rev. A* **78** 061802
[9] Erkmen B I 2012 *J. Opt. Soc. Am. A* **29** 782
[10] Zhao C, Gong W, Chen M, Li E, Wang H, Xu W and Han S 2012 *Appl. Phys. Lett.* **101** 141123
[11] Gong W and Han S 2015 *Sci. Rep.* **5** 9280
[12] Zhao S M and Zhuang P 2014 *Chin. Phys. B* **23** 054203
[13] Yu W, Li M, Yao X, Liu X, Wu L and Zhai G 2014 *Opt. Express* **22** 7133
[14] Cheng J 2009 *Opt. Express* **17** 7916
[15] Zhang P, Gong W, Shen X and Han S 2010 *Phys. Rev. A* **82** 033817
[16] Hardy N D and Shapiro J H 2011 *Phys. Rev. A* **84** 063824
[17] Gong W and Han S 2011 *Opt. Lett.* **36** 394
[18] Tajahuerce E, Duran V, Clemente P, Irles E, Soldevila F, Andres P and Lancis J 2014 *Opt. Express* **22** 16945
[19] Yang Z, Zhao L, Zhao X, Qin W and Li J 2016 *Chin. Phys. B* **25** 024202
[20] Bina M, Magatti D, Moltini M, Gatti A, Lugiato L A and Ferri F 2013 *Phys. Rev. Lett.* **110** 083901
[21] Gao L, Liu X L, Zheng Z and Wang K 2014 *J. Opt. Soc. Am. A* **31** 886
[22] Wang C, Zhang D, Bai Y and Chen B 2010 *Phys. Rev. A* **82** 063814
[23] Nan S, Bai Y, Shi X, Shen Q, Li H, Qu L and Fu X 2017 *IEEE Photonics J.* **9** 7500107
[24] Nan S, Bai Y, Shi X, Shen Q, Qu L, Li H and Fu X 2017 *Photonics Res.* **5** 372
[25] Hardy N D and Shapiro J H 2013 *Phys. Rev. A* **87** 023820
[26] Yu H, Li E, Gong W and Han S 2015 *Opt. Express* **23** 14541
[27] Gong W, Zhao C, Yu H, Chen M, Xu W and Han S 2016 *Sci. Rep.* **6** 26133
[28] Deng C, Pan L, Wang C, Gao X, Gong W and Han S 2017 *Photonics Res.* **5** 431
[29] Chan K W C, O'Sullivan M N and Boyd R W 2009 *Phys. Rev. A* **79** 033808
[30] Karmakar S and Shih Y 2010 *Phys. Rev. A* **81** 033845
[31] Shi D, Fan C, Zhang P, Shen H, Zhang J, Qiao C and Wang Y 2013 *Opt. Express* **21** 2050
[32] Zhang D J, Li H G, Zhao Q L, Wang S, Wang H B, Xiong J and Wang K 2015 *Phys. Rev. A* **92** 013823
[33] Cheng J and Han S 2007 *Phys. Rev. A* **76** 023824
[34] Shen Q, Bai Y, Shi X, Nan S, Qu L, Li L and Fu X 2018 *Laser Phys. Lett.* **15** 035207
[35] Mandel L and Wolf E 1995 *Optical Coherence and Quantum Optics* (Cambridge University Press)
[36] Hu F, Wang X and Zhang J 2005 *Infrared Technol.* **2** 008